AIMS Mathematics, 10(9): 20979–21003.
DOI:10.3934/math.2025937
Received: 19 May 2025
Revised: 17 August 2025
Accepted: 21 August 2025
Published: 12 September 2025

https://www.aimspress.com/journal/Math

Research article

Embankment surfaces with the Darboux frame in Euclidean 3-space

Erdem Kocakuşaklı[1,2,*]

[1] Department of Mathematics, Faculty of Arts and Science, Sinop University, Sinop, Turkey
[2] Department of Basic Sciences, Turkish Military Academy, National Defense University, Ankara, Turkey

* **Correspondence:** Email: ekocakusakli@sinop.edu.tr, erdem.kocakusakli@msu.edu.tr.

Abstract: This article was dedicated to the study of embankment, embankment-like, and tubembankment-like surfaces generated by a regular space curve according to the Darboux frame in Euclidean 3-space. Initially, we presented the parametric equations defining these surfaces. Subsequently, their quaternionic and matrix representations were derived to provide alternative and efficient formulations. In addition, the geometric properties of tubembankment-like surfaces were thoroughly examined, leading to several significant theorems and corollaries. To demonstrate the applicability and validity of the theoretical results, illustrative examples were generated by using the Mathematica program.

Keywords: embankment surface; Darboux frame; quaternion; matrix representation; homothetic motion
Mathematics Subject Classification: 53A05, 53A17, 53A55

1. Introduction

Surfaces of revolution hold a very important place in geometry. Ruled surfaces, canal surfaces, and embankment surfaces belong to this class of surfaces. Ruled surfaces from this family are generated by moving a line along a curve. Canal and embankment surfaces are constructed by the movement of spheres and cones along a curve, respectively.

Ruled surfaces are important from a geometric point of view. Many mathematicians have provided parametrizations of these surfaces according to the Frenet frames of curves and examined their geometric properties. These surfaces were first introduced and studied by Monge [1]. Catalan studied ruled minimal surfaces [2]. The theory of ruled surfaces was further developed by using the E-Study transformation [3]. The geometric properties of the ruled surfaces were investigated by Izumiya and Takachi [4]. Similarly, Yoon [5] investigated the characterization and properties of ruled surfaces.

Another important family of surfaces are canal surfaces defined by Monge [6]. The canal surface is generated as the envelope of a moving sphere with variable radius. It is a special case where the tubular surface has a constant radius. Canal surfaces and tubular surfaces have been studied extensively in geometry. Gray mentioned canal surfaces and their equations, illustrating their graphs using the program Mathematica [7]. Gross studied canal surfaces from an analytical perspective [8]. Uçum and İlarslan also examined canal surfaces from a different point of view [9]. Xu investigated the analytical and algebraic properties of canal surfaces [10]. Karacan explored Weingarten-type tubular surfaces and geodesics of tubular surfaces, considering them from a geometrical perspective in certain spaces [11, 12]. Maekawa and others analyzed tubular surfaces, which are special cases of canal surfaces, and studied some of their applications [13]. Blaga examined tubular surfaces in computer graphics [14]. Canal and tubular surfaces are very useful in engineering and computer visualization. Moreover, these surfaces have many applications in daily life.

Especially for curves, geometric properties are examined using the Frenet frame. However, this frame may not be defined for all points along every curve. The Bishop, Darboux, and extending Darboux frames provide the desired properties for space curves. Therefore, they are important in areas such as mathematical analysis and computer graphics. In recent years, these frames have been widely used, especially in curve and surface theory. Some significant works on curves and surfaces according to the Darboux frame are also presented [15–18].

Parametric expressions of surfaces generated by movements along a curve can be succinctly expressed with the help of homothetic motions and matrices. In addition, quaternions defined by Hamilton, have a very useful structure in terms of representing movements [19]. Thus, surface equations can be expressed more simply with the aid of quaternions corresponding to matrices. Quaternions, which hold an important place in the geometry of motion, are widely used, especially in terms of expressing surfaces more easily and providing operational convenience. Detailed information, applications, and examples on this subject are given in [20] and [21]. Babaarslan and Yaylı examined constant slope surfaces using quaternions [22]. Aslan and Yaylı expressed canal surfaces generated by a regular curve with quaternions and investigated and exemplified their properties using the Darboux frame in the Euclidean 3-space [23]. Then, Gök examined canal and tubular surfaces constructed by spherical indicatrices of regular curves with an alternative moving frame in Euclidean 3-Space. Moreover, he provided their matrix and quaternionic representations [24]. Doğan characterized canal surfaces in different frames, including the Darboux frame, and investigated their properties within this frame [15, 25]. Ateş et al. examined tubular surfaces constructed by spherical indicatrices of a regular curve with an alternative moving frame in the Euclidean 3-Space [26]. They presented some properties satisfied by these tubular surfaces and provided related examples.

Similarly to canal and tubular surfaces, embankment surfaces are also defined [27]. The embankment surface is generated by the envelope of a moving cone of variable radius. Since its parametrization depends on its own components, it is difficult to express. For this reason, embankment-like surfaces created based on an arbitrary function and tubembankment-like surfaces created with the help of a constant function are defined.

Embankment surfaces can be modeled by using parametric methods. These surfaces have found significant usage and application areas, especially in geological engineering. They play a highly functional role in infrastructure projects such as terrain modeling, road construction, and dam design. They are employed in these structures to prevent landslides. Furthermore, derivation of geometric

equations is important for facilating the construction of these structures. Thanks to their parametric definitions, geometric properties such as slope, curvature, and local orientation can be precisely controlled. Thus, critical engineering factors such as the stability of embankments or support structures, material optimization, and drainage analysis can be examined more effectively. In addition, digital modeling of these surfaces enables rapid prototyping and simulation processes within GIS (geographic information systems)- and CAD (computer aided design)-based terrain design systems. In this way, it contributes to reducing project costs and increasing design accuracy. Therefore, the application of embankment surfaces plays an effective role for both theoretical geometry studies and practical engineering designs. Detailed information on engineering applications, usage areas, and the importance of these surfaces is provided in the study titled "Guidelines for Embankment Construction" [28].

However, while many articles deal with the geometric aspects of canal and tubular surfaces, embankment surfaces have been studied very little. One of the most important works in this area is the study conducted by Kazan and Karadağ [29]. They investigated embankment, embankment-like and tubembankment-like surfaces constructed by regular curves in Euclidean 3-Space. Moreover, they provided quaternionic representations and some properties of these surfaces. Finally, each surface was exemplified, and their graphs were drawn by using Mathematica. Another important article dealing with these surfaces from a geometrical perspective is the work done by Mahmoud and Abd ElHafez [30]. In this study, they considered and characterized the isotropic Weingarten embankment surfaces. They presented their geometrical properties and illustrated the graphs by providing examples for each surface.

In the classical differential geometry literature, canal and tubular surfaces generated by envelope families of spheres along a space curve have been studied, and their properties investigated both in Euclidean space and, where problems arise or to provide a different perspective, in Bishop, Darboux, and alternative moving frames. Similarly, embankment and embankment-like surfaces generated by envelope families of cones have received very little study, almost exclusively in Euclidean and Galilean spaces. In these studies, quaternionic expressions have been given and exemplified. However, studies particularly in Euclidean space, other than those based on the Frenet frame, are scarce. In particular, in derivative calculations, applying rotations locally at points where problems arise is more easily achieved with alternative moving frames. Bishop and Darboux frames are among these alternative frames. To contribute to addressing this deficiency in the literature, in this paper, we specifically address the surfaces generated by envelope families of cone surfaces in the Darboux frame. This motivation has led us to undertake the present study.

The rest of the paper is organized as follows: Section 2 presents the general definitions employed in differential geometry, together with the Darboux frame and its properties. Quaternions and their properties are then introduced, along with their corresponding matrix representations, which play a significant role in the geometry of motion. In Section 3, embankment surfaces are defined with respect to the Darboux frame and expressed parametrically; subsequently, simpler representations are obtained via quaternions, and their matrix counterparts are formulated as homothetic motions. Section 4 follows a similar approach for embankment-like surfaces, constructed in terms of the Darboux frame elements and represented using quaternions, with their equations derived through matrix representations. Section 5 addresses tubembankment-like surfaces, the most specific case of embankment surfaces, again defined with respect to the Darboux frame. Their equations are obtained in a concise form using

quaternions and matrices, followed by the computation of the normal vector, fundamental form coefficients, and curvature functions. Several results and theorems characterizing these surfaces are presented, and the conditions under which their parameter curves become special curves are examined, contributing to the closure of certain gaps in the literature. The minimal curve conditions are also determined, showing that such surfaces are Weingarten surfaces. In Section 6, embankment-like and tubembankment-like surfaces are generated from a curve according to the Darboux frame, and their parametric, quaternionic, and matrix representations are provided. Examples and applications are of great importance in geometry. Therefore, graphical illustrations of these surfaces under various parameter settings are produced using Mathematica. As analytical equations of surfaces alone may be insufficient for a full understanding of their geometric properties, three-dimensional visualization offers a clear means of observing their structural characteristics, thereby serving as a powerful tool for both theoretical and applied analyses. Finally, Section 7 summarizes the main conclusions of this work.

2. Background material

Let $\mathbb{E}^3$ be 3-dimensional Euclidean space endowed with the standard metric given by

$$\langle \vec{u}, \vec{v} \rangle = \vec{u}_1\vec{v}_1 + \vec{u}_2\vec{v}_2 + \vec{u}_3\vec{v}_3,$$

where $\vec{u} = (u_1, u_2, u_3), \vec{v} = (v_1, v_2, v_3) \in \mathbb{R}^3$. The norm of the vector $u \in \mathbb{R}^3$ is defined by

$$\left\|\vec{u}\right\| = \sqrt{\langle \vec{u}, \vec{u} \rangle},$$

and the vector product is given by

$$\vec{u} \wedge \vec{v} = (u_2v_3 - v_2u_3, u_3v_1 - v_3u_1, u_1v_2 - v_1u_2)$$

[31].

We recall elementary properties of the surface in $\mathbb{R}^3$.

The Gauss map of the surface $\Psi(s, \theta)$ is the following as:

$$\vec{U} = \frac{\Psi_s \wedge \Psi_\theta}{\|\Psi_s \wedge \Psi_\theta\|},$$

where $\{\Psi_s, \Psi_\theta\}$ is the natural base [31].

Then, the first fundamental form **I** and the second fundamental form **II** of the surface $\Psi(s, \theta)$ are defined by

$$\begin{aligned} \mathbf{I} &= g_{11}ds^2 + 2g_{12}dsd\theta + g_{22}d\theta^2, \\ \mathbf{II} &= L_{11}ds^2 + 2L_{12}dsd\theta + L_{22}d\theta^2, \end{aligned}$$

respectively [31], where we put

$$\begin{aligned} g_{11} &= \langle \Psi_s, \Psi_s \rangle, g_{12} = \langle \Psi_s, \Psi_\theta \rangle, g_{22} = \langle \Psi_\theta, \Psi_\theta \rangle, \\ L_{11} &= \left\langle \Psi_{ss}, \vec{U} \right\rangle, L_{12} = \left\langle \Psi_{s\theta}, \vec{U} \right\rangle, L_{22} = \left\langle \Psi_{\theta\theta}, \vec{U} \right\rangle. \end{aligned}$$

We can compute Gauss and mean curvature functions as, respectively

$$K = \frac{L_{11}L_{22} - L_{12}^2}{g_{11}g_{22} - g_{12}^2}, H = \frac{g_{22}L_{11} - 2g_{12}L_{12} + g_{11}L_{22}}{2(g_{11}g_{22} - g_{12}^2)}.$$

We know that a surface is called a (H, K)-Weingarten surface if it satisfies $\Phi(H, K) = H_s K_\theta - H_\theta K_s = 0$ [32].

Let $\alpha : I \subset \mathbb{R} \to \mathbb{E}^3$ be a regular unit speed curve with Frenet apparatus $\left\{\vec{T}(s), \vec{N}(s), \vec{B}(s), \kappa(s), \tau(s)\right\}$ in Euclidean space $\mathbb{E}^3$. Here, $\kappa(s)$ and $\tau(s)$ are called the first and the second curvature functions of the curve $\alpha(s)$, respectively.

Since the curve $\alpha(s)$ also lies on the surface $\Psi(s, \theta)$, there exists another frame along $\alpha(s)$ which is called the Darboux frame and given by $\left\{\vec{T}(s), \vec{g}(s), \vec{n}(s)\right\}$. In this frame, $\vec{T}(s)$ is the unit tangent of the curve $\alpha(s)$, $\vec{n}(s)$ is the unit normal of the surface $\Psi(s, \theta)$ along the curve $\alpha(s)$, and $\vec{g}(s)$ is a unit vector defined by $\vec{g} = \vec{n} \wedge \vec{T}$.

We can give the following relation for Frenet and Darboux frame apparatus:

$$\begin{bmatrix} \vec{T}(s) \\ \vec{g}(s) \\ \vec{n}(s) \end{bmatrix} = \begin{bmatrix} 1 & 0 & 0 \\ 0 & \cos\Theta(s) & \sin\Theta(s) \\ 0 & -\sin\Theta(s) & \cos\Theta(s) \end{bmatrix} \begin{bmatrix} \vec{T}(s) \\ \vec{N}(s) \\ \vec{B}(s) \end{bmatrix}, \tag{2.1}$$

where Θ is the angle between the vectors $\vec{g}(s)$ and $\vec{N}(s)$.

The derivatives of the Darboux frame are given by the following formulae:

$$\begin{bmatrix} \vec{T}'(s) \\ \vec{g}'(s) \\ \vec{n}'(s) \end{bmatrix} = \begin{bmatrix} 0 & \kappa_g(s) & \kappa_n(s) \\ -\kappa_g(s) & 0 & \tau_g(s) \\ -\kappa_n(s) & -\tau_g(s) & 0 \end{bmatrix} \begin{bmatrix} \vec{T}(s) \\ \vec{g}(s) \\ \vec{n}(s) \end{bmatrix}, \tag{2.2}$$

where $\kappa_g(s) = \kappa(s)\cos\Theta(s)$, $\kappa_n(s) = \kappa(s)\sin\Theta(s)$, and $\tau_g(s) = \tau(s) + \frac{d\Theta}{ds}$.

Moreover, the geodesic curvature $\kappa_g(s)$ and geodesic torsion $\tau_g(s)$ of the curve $\alpha(s)$ can be calculated as

$$\kappa_g = \left\langle \frac{d\alpha}{ds}, \frac{d^2\alpha}{ds^2} \wedge \vec{n} \right\rangle, \ \tau_g = \left\langle \frac{d\alpha}{ds}, \vec{n} \wedge \frac{d\vec{n}}{ds} \right\rangle.$$

In the differential geometry of surfaces, for a surface curve $\alpha(s)$, the following is well-known:

i) $\alpha(s)$ is a geodesic curve if, and only if, $\kappa_g = 0$,

ii) $\alpha(s)$ is an asymptotic line if, and only if, $\kappa_n = 0$,

iii) $\alpha(s)$ is a principal line if, and only if, $\tau_g = 0$ (see [31, 33, 34] for details).

The real quaternion algebra $\mathbb{H}$ was consicely defined by Hamilton [19] in the following form:

$$\mathbb{H} = \{Q = q_0 + q_1 i + q_2 j + q_3 k \mid q_0, q_1, q_2, q_3 \in \mathbb{R}\},$$

where i, j, k are imaginary units satisfying the following multiplication rules:

$$i^2 = j^2 = k^2 = i \wedge j \wedge k = -1, i \wedge j = -j \wedge i = k.$$

This real quaternion algebra is associative and not commutative. A basis of real quaternions is $\{1, i, j, k\}$ and the identity element of $\mathbb{H}$ is 1. Also, i, j, and k are standard orthonormal bases in $\mathbb{R}^3$. A

real quaternion can be written as $Q = q_0 + q_1 i + q_2 j + q_3 k$ or $Q = (q_0, \vec{v})$, where the vector and the scalar component of Q are $V(Q) = \vec{v} \in \mathbb{R}^3$ and $S(Q) = q_0 \in \mathbb{R}$, respectively. So, the real quaternion can be written as $Q = S(Q) + V(Q)$. If $S(Q) = 0$, the real quaternion is called a pure real quaternion. The conjugate of a real quaternion, addition of two real quaternions, and multiplication of a real quaternion with a scalar λ can be given, respectively, as

$$\begin{aligned} \overline{Q} &= S(Q) - V(Q), \\ Q + P &= (S(Q) + S(P)) + (V(Q) + V(P)), \\ \lambda Q &= \lambda S(Q) + \lambda V(Q). \end{aligned}$$

By using dot and cross-product, we can give the real quaternion product of two real quaternions Q and P as

$$Q \times P = S(Q)S(P) - < V(Q), V(P) > + S(Q)V(P) + S(P)V(Q) + V(Q) \wedge V(P), \tag{2.3}$$

where $\times$ is the real quaternion product. The norm of a real quaternion is $|Q|^2 = Q \times \overline{Q} = \overline{Q} \times Q$ and $|Q| = \sqrt{q_0^2 + q_1^2 + q_2^2 + q_3^2}$. If norm of a real quaternion is 1, it is called a unit real quaternion. The unit real quaternion can be written as $Q = cos\frac{\theta}{2} + \sin\frac{\theta}{2}\vec{v}$, where $\vec{v} \in \mathbb{R}^3$ and $\left\|\vec{v}\right\| = 1$ The inverse of Q can be given as

$$Q^{-1} = \frac{\overline{Q}}{|Q|^2}, \ |Q| \neq 0.$$

One parameter homothetic motion in the 3-dimensional Euclidean space can be given by the following translation as

$$y = h\mathcal{M}_Q x + C,$$

where y and x are the position vectors of a same point of the fixed space R' and the moving space R, respectively. h, $\mathcal{M}_Q$, and C are a homothetic scalar, an orthogonal matrix, and a translation vector, respectively; also, they are continuously differentiable functions dependent on real parameter s.

Let $\phi : \mathbb{R}^3 \to \mathbb{R}^3$ be a linear mapping and $\phi(\vec{u}) = Q \times \vec{u} \times Q^{-1}$, where Q is a unit real quaternion and $\vec{u}$ is a pure real quaternion (a vector in $\mathbb{R}^3$). So, for every unit real quaternion $Q = q_0 + q_1 i + q_2 j + q_3 k$, we can give matrix representation $\mathcal{M}_Q$ of ϕ by using pure real quaternion basis elements of $\mathbb{H}$ as

$$\mathcal{M}_Q = \begin{bmatrix} q_0^2 + q_1^2 - q_2^2 - q_3^2 & -2q_0q_3 + 2q_1q_2 & 2q_0q_2 + 2q_1q_3 \\ 2q_0q_3 + 2q_1q_2 & q_0^2 + q_2^2 - q_1^2 - q_3^2 & -2q_0q_1 + 2q_2q_3 \\ -2q_0q_2 + 2q_1q_3 & 2q_0q_1 + 2q_2q_3 & q_0^2 + q_3^2 - q_1^2 - q_2^2 \end{bmatrix}, \tag{2.4}$$

where $\mathcal{M}_Q$ is an orthogonal matrix (namely $\mathcal{M}_Q M_Q^T = I$ and $det\mathcal{M}_Q = 1$) [21]. Thus, we can say that the linear mapping ϕ is a rotation in 3-dimensional space. Additionally, ϕ is given as
$\phi(\vec{u}) = Q \times \vec{u} \times Q^{-1} = \mathcal{M}_Q u$.

The vector $\vec{u}(s)$ is consistently treated as a 3×1 column matrix representing the expression denoted by u in matrix multiplications. It is considered as a pure real quaternion in quaternion multiplications.

3. Embankment surfaces according to the Darboux frame in $\mathbf{E}^3$

In this section, the definitions required for the construction of embankment surfaces will first be presented, and then the equations of these surfaces with respect to the Darboux frame will be derived with detailed step by step procedures. Subsequently, the surface equations will be expressed in terms of homothetic motions using matrices and quaternions multiplications.

Let $\Lambda : (r(t), z(t))$, $t \in [a, b]$ be a parametric planar curve with $r > 0$, then $\Phi := (r(t)\cos\varphi, r(t)\sin\varphi, z(t))$, $t \in [a, b]$, $\varphi \in [0, 2\pi]$ is called parametric surface of revolution. For any implicit planar curve $\Lambda : f(r, z) = 0$ with $r > 0$, the surface $\Phi := \left(\sqrt{x^2 + y^2}, z\right)$ is called implicit surface of revolution [27].

Let $\Phi_c : f(X, c) = 0$, $c \in [c_1, c_2]$ be a one parameter family of regular implicit surfaces. The intersection curve of two neighbored surfaces Φ_c and $\Phi_{c+\Delta c}$ fulfills the two equations $f(X, c) = 0$ and $f(X, c + \Delta c) = 0$. We consider the limit for $\Delta c \to 0$ and get $f_c(X, c) = \lim_{\Delta c \to 0} \frac{f(X, c) - f(X, c + \Delta c)}{\Delta c} = 0$ [27]. The last equation motivates the following definitions.

Definition 3.1. Let $\Phi_c : f(X, c) = 0$, $c \in [c_1, c_2]$ be a one parameter family of regular implicit C^2 surfaces. The surface which is defined by the two equations $f(X, c) = 0$ and $f_c(X, c) = 0$ is called envelope of the given family of surfaces [27].

Definition 3.2. Let $\Lambda : X = \alpha(s) = (\alpha_1(s), \alpha_2(s), \alpha_3(s))$ be a regular space curve and $m \in \mathbb{R}$, $m > 0$ with $\left|m\alpha_3'\right| < \sqrt{\left(\alpha_1'\right)^2 + \left(\alpha_2'\right)^2}$. Then, the envelope of the one parameter family of cones

$$f(X; s) := (x - \alpha_1(s))^2 + (y - \alpha_2(s))^2 - m^2 (z - \alpha_3(s))^2 = 0 \tag{3.1}$$

is called an embankment surface and Λ is its directrix [27].

In Definition 3.2, the condition $\left|m\alpha_3'\right| < \sqrt{\left(\alpha_1'\right)^2 + \left(\alpha_2'\right)^2}$ guarantees an intersection with the cone. For more detailed information, see ([27], p.118).

The stages of creating embankment surfaces that are constructed by a regular space curve can be seen in Figure 1 [27]. The embankment surfaces are generated through envelope families of cones moving along the curve. Figure 1(a) depicts the motion of a cone along the curve. Figure 1(b) illustrates the formation process of the envelope families of these cones. Figure 1(c) presents the resulting embankment surfaces, namely, the envelopes of cones moving along the curve.

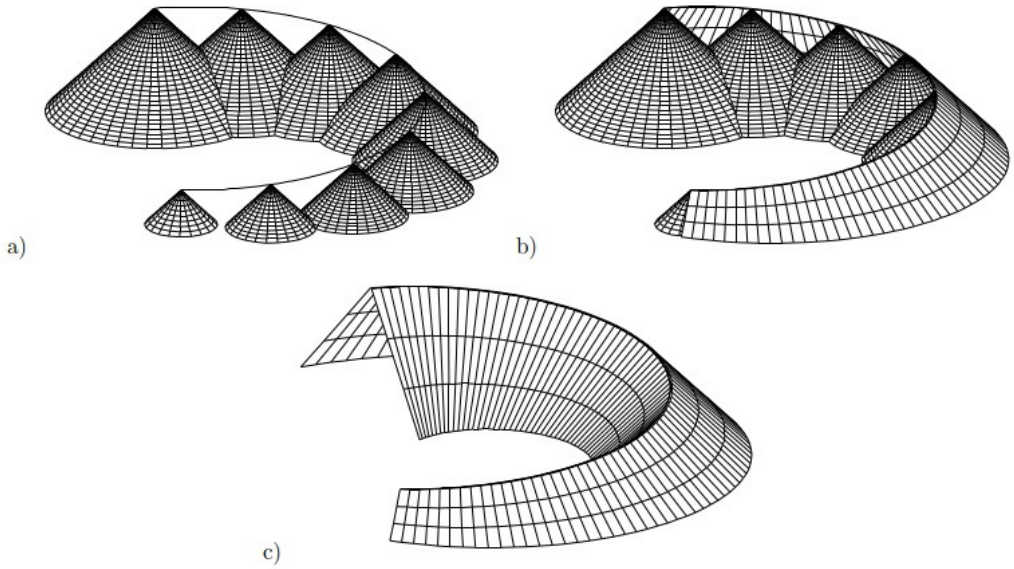

Figure 1. Generation of an embankment surface.

Let Ψ^E be a parametrization of the envelope of cones defining the embankment surface given by $\Psi^E(s,\theta) = \left(\Psi^{E_1}(s,\theta), \Psi^{E_2}(s,\theta), \Psi^{E_3}(s,\theta)\right)$. Moreover, let $\alpha(s) = (\alpha_1(s), \alpha_2(s), \alpha_3(s))$ be a regular space curve which is diretrix of $\Psi^E(s,\theta)$ and $m \in \mathbb{R}$, $m > 0$ with $\left|m\alpha_3'\right| < \sqrt{\left(\alpha_1'\right)^2 + \left(\alpha_2'\right)^2}$. Then, the embankment surface can be given as

$$\begin{aligned}\left(\Psi^{E_1}(s,\theta) - \alpha_1(s)\right)^2 + \left(\Psi^{E_2}(s,\theta) - \alpha_2(s)\right)^2 - m^2\left(\Psi^{E_3}(s,\theta) - \alpha_3(s)\right)^2 \\ + \left(\Psi^{E_3}(s,\theta) - \alpha_3(s)\right)^2 - \left(\Psi^{E_3}(s,\theta) - \alpha_3(s)\right)^2 = 0.\end{aligned} \tag{3.2}$$

In the next step, the following equality is obtained by making the necessary adjustments to Eq (3.2).

$$\left\langle \Psi^E(s,\theta) - \alpha(s), \Psi^E(s,\theta) - \alpha(s) \right\rangle = \left(m^2+1\right)\left(\Psi^{E_3}(s,\theta) - \alpha_3(s)\right)^2. \tag{3.3}$$

However, the parametric equation on this surface with Darboux frame is given as

$$\Psi^E(s,\theta) - \alpha(s) = a_1(s,\theta)\vec{T}(s) + a_2(s,\theta)\vec{g}(s) + a_3(s,\theta)\vec{n}(s), \tag{3.4}$$

where a_1, a_2, and a_3 are differentiable functions of s and θ on the interval I.

Moreover, we have

$$\left\langle \Psi^E(s,\theta) - \alpha(s), \Psi^E(s,\theta) - \alpha(s) \right\rangle = a_1^2(s,\theta) + a_2^2(s,\theta) + a_3^2(s,\theta). \tag{3.5}$$

Hence, via (3.3) and (3.5), we have

$$a_1^2(s,\theta) + a_2^2(s,\theta) + a_3^2(s,\theta) = \left(m^2+1\right)\left(\Psi^{E_3}(s,\theta) - \alpha_3(s)\right)^2. \tag{3.6}$$

By taking the derivative of expression (3.6) with respect to s and θ, the subsequent Eqs (3.7) and (3.8) are obtained, respectively.

$$a_1(s,\theta)a_1(s,\theta)_s+a_2(s,\theta)a_2(s,\theta)_s+a_3(s,\theta)a_3(s,\theta)_s = (m^2+1)\left(\Psi^{E_3}(s,\theta)-\alpha_3(s)\right)\left(\Psi^{E_3}(s,\theta)-\alpha_3(s)\right)_s. \tag{3.7}$$

$$a_1(s,\theta)\,a_1(s,\theta)_\theta + a_2(s,\theta)\,a_2(s,\theta)_\theta + a_3(s,\theta)\,a_3(s,\theta)_\theta = \left(m^2+1\right)\left(\Psi^{E_3}(s,\theta)-\alpha_3(s)\right)\left(\Psi^{E_3}(s,\theta)\right)_\theta. \tag{3.8}$$

Also, if we differentiate the Eq (3.4) with respect to s and θ, then, we have

$$\begin{aligned}\Psi^E_s(s,\theta) &= \left(\|\alpha'(s)\| + a_1(s,\theta)_s - \kappa_g a_2(s,\theta) - \kappa_n a_3(s,\theta)\right)\vec{T}(s) \\ &+ \left(a_2(s,\theta)_s + \kappa_g a_1(s,\theta) - a_3(s,\theta)\,\tau_g\right)\vec{g}(s) \\ &+ \left(a_3(s,\theta)_s + \kappa_n a_1(s,\theta) - \tau_g a_2(s,\theta)\right)\vec{n}(s),\end{aligned} \tag{3.9}$$

and

$$\Psi^E_\theta(s,\theta) = a_1(s,\theta)_\theta\,\vec{T}(s) + a_2(s,\theta)_\theta\,\vec{g}(s) + a_3(s,\theta)_\theta\,\vec{n}(s). \tag{3.10}$$

Since the embankment surfaces and cones are tangent to each other along the curve, their tangent planes at the contact points coincide. As the position vector of the cone equals to its normal vector, the normal of the cone surface is given by

$$\vec{U}(s,\theta) = \Psi^E(s,\theta) - \alpha(s).$$

Therefore, the condition

$$\left\langle \Psi^E(s,\theta)-\alpha(s), \Psi^E_s(s,\theta)\right\rangle = 0$$

constitutes a necessary and sufficient condition for the embankment surface. Next, using Eqs (3.4) and (3.9), we arrive at the following result:

$$a_1(s,\theta)\,\|\alpha'(s)\| + a_1(s,\theta)\,a_1(s,\theta)_s + a_2(s,\theta)\,a_2(s,\theta)_s + a_3(s,\theta)\,a_3(s,\theta)_s = 0. \tag{3.11}$$

Hence, by using (3.7) and (3.11), we obtain

$$a_1(s,\theta) = -\frac{\left(m^2+1\right)}{\|\alpha'(s)\|}\left(\Psi^{E_3}(s,\theta)-\alpha_3(s)\right)\left(\Psi^{E_3}(s,\theta)-\alpha_3(s)\right)_s. \tag{3.12}$$

By utilizing Eqs (3.6) and (3.12), the following expression can be derived.

$$a_2^2(s,\theta)+a_3^2(s,\theta) = \left(m^2+1\right)\left(\Psi^{E_3}(s,\theta)-\alpha_3(s)\right)^2\left(1-\frac{\left(m^2+1\right)}{\|\alpha'(s)\|^2}\left(\Psi^{E_3}(s,\theta)-\alpha_3(s)\right)_s^2\right). \tag{3.13}$$

With the help of (3.13), and using the well-known fundamental trigonometric identity $\cos^2\theta+\sin^2\theta = 1$, the following selections can be made.

$$\begin{aligned}a_2(s,\theta) &= \pm\sqrt{m^2+1}\left(\Psi^{E_3}(s,\theta)-\alpha_3(s)\right)\sqrt{1-\frac{(m^2+1)}{\|\alpha'(s)\|^2}\left(\Psi^{E_3}(s,\theta)-\alpha_3(s)\right)_s^2}\cos\theta, \\ a_3(s,\theta) &= \pm\sqrt{m^2+1}\left(\Psi^{E_3}(s,\theta)-\alpha_3(s)\right)\sqrt{1-\frac{(m^2+1)}{\|\alpha'(s)\|^2}\left(\Psi^{E_3}(s,\theta)-\alpha_3(s)\right)_s^2}\sin\theta.\end{aligned} \tag{3.14}$$

So, we can construct our main theorem as the following:

Theorem 3.3. *In Euclidean 3-space E^3, an embankment surface is the envelope of a one-parameter family of cones centered on the spine curve $\alpha(s)$. The embankment surface can be parametrized as*

$$\begin{aligned}\Psi^E(s,\theta) &= \alpha(s) - \frac{m^2+1}{\|\alpha'(s)\|}\sigma_3(s,\theta)\,\sigma_3(s,\theta)_s\,\vec{T}(s) \\ &\pm \sqrt{m^2+1}\sigma_3(s,\theta)\sqrt{1-\frac{(m^2+1)}{\|\alpha'(s)\|^2}\sigma_3(s,\theta)_s^2}(\cos\theta\vec{g}(s)+\sin\theta\vec{n}(s)),\end{aligned} \tag{3.15}$$

where $\left\{\vec{T},\vec{g},\vec{n}\right\}$ is the Darboux frame of $\alpha(s)$, $\sigma_3(s,\theta) = \Psi^{E_3}(s,\theta) - \alpha_3(s)$, and $m \in \mathbb{R}$, $m > 0$ with $\left|m\alpha_3'\right| < \sqrt{\left(\alpha_1'\right)^2 + \left(\alpha_2'\right)^2}$.

Theorem 3.4. *Let $\alpha : I \subset \mathbb{R} \to \mathbb{R}^3$ be a unit speed diretrix curve of embankment surface $\Psi^E(s,\theta)$ and $Q(s,\theta) = cos\frac{\theta}{2} + \sin\frac{\theta}{2}\vec{T}(s)$ be a unit real quaternion in $S^3 \subset \mathbb{R}^4$. Then, the parametric equation of embankment surface $\Psi^E(s,\theta)$ generated by the curve α can be given*

(i) Via the real quaternion product $Q(s,\theta)\times\vec{g}(s)\times Q^{-1}(s,\theta)$

$$\begin{aligned}\Psi^E(s,\theta) &= \alpha(s) - \left(m^2+1\right)\sigma_3(s,\theta)\,\sigma_3(s,\theta)_s\,\vec{T}(s) \\ &\pm \sqrt{m^2+1}\sigma_3(s,\theta)\sqrt{1-(m^2+1)\,\sigma_3(s,\theta)_s^2}\,Q(s,\theta)\times\vec{g}(s)\times Q^{-1}(s,\theta).\end{aligned} \tag{3.16}$$

(ii) Via the matrix representation of the map $\phi : \mathbb{R}^3 \to \mathbb{R}^3$ for the unit real quaternion $Q(s,\theta)$ and $\Psi^E(s,\theta)$ can be obtained by the homothetic motion as

$$\begin{aligned}\Psi^E(s,\theta) &= \alpha(s) - \left(m^2+1\right)\sigma_3(s,\theta)\,\sigma_3(s,\theta)_s\,\vec{T}(s) \\ &\pm \sqrt{m^2+1}\sigma_3(s,\theta)\sqrt{1-(m^2+1)\,\sigma_3(s,\theta)_s^2}\,\mathcal{M}_Q g,\end{aligned} \tag{3.17}$$

where $\left\{\vec{T},\vec{g},\vec{n}\right\}$ is the Darboux frame of $\alpha(s)$, $\mathcal{M}_Q$ is the matrix representation of the map ϕ for $Q(s,\theta)$, $\sigma_3(s,\theta) = \Psi^{E_3}(s,\theta) - \alpha_3(s)$, and $m \in \mathbb{R}$, $m > 0$ with $\left|m\alpha_3'\right| < \sqrt{\left(\alpha_1'\right)^2 + \left(\alpha_2'\right)^2}$.

Proof. Assume that $\Psi^E(s,\theta)$ is an embankment surface generated by the unit speed curve $\alpha(s)$ according to the orthonormal Darboux frame $\left\{\vec{T},\vec{g},\vec{n}\right\}$. By using (3.15), we can easily obtain

$$\begin{aligned}\Psi^E(s,\theta) &= \alpha(s) - \left(m^2+1\right)\sigma_3(s,\theta)\,\sigma_3(s,\theta)_s\,\vec{T}(s) \\ &\pm \sqrt{m^2+1}\sigma_3(s,\theta)\sqrt{1-(m^2+1)\,\sigma_3(s,\theta)_s^2}(\cos\theta\vec{g}(s)+\sin\theta\vec{n}(s)).\end{aligned}$$

Via (2.3), for the real quaternions $Q(s,\theta) = cos\frac{\theta}{2} + \sin\frac{\theta}{2}\vec{T}(s)$, $Q^{-1}(s,\theta) = cos\frac{\theta}{2} - \sin\frac{\theta}{2}\vec{T}(s)$ and the pure real quaternion $\vec{g}(s)$, we get

$$Q(s,\theta)\times\vec{g}(s)\times Q^{-1}(s,\theta) = \cos\theta\vec{g}(s) + \sin\theta(\vec{T}(s)\wedge\vec{g}(s)) + (1-\cos\theta) < \vec{T}(s),\vec{g}(s) > \vec{T}(s).$$

The trigonometric half-angle formulas are employed here.

As a result, since the coefficients of the Darboux frame are orthogonal, their inner products are zero. Consequently, the following equality is obtained.

$$Q(s,\theta)\times\vec{g}(s)\times Q^{-1}(s,\theta)=\cos\theta\vec{g}(s)+\sin\theta\vec{n}(s). \tag{3.18}$$

On the other hand, if $\alpha(s) - \left(m^2+1\right)\sigma_3(s,\theta)\,\sigma_3(s,\theta)_s\,\vec{T}(s)$, $\pm\sqrt{m^2+1}\sigma_3(s,\theta)\sqrt{1-(m^2+1)\,\sigma_3(s,\theta)_s^2}$, and $\mathcal{M}_Q$ are defined as translation vector, the homothetic scalar, and the orthogonal matrix of the homothetic motion, respectively, then (3.17) is a homothetic motion. This completes the proof. □

4. Embankment-like surfaces according to the Darboux frame in $\mathbf{E}^3$

In this section, first, embankment-like surfaces, which are special cases of embankment surfaces, will be defined. Subsequently, the parametric equations of these surfaces according to the Darboux frame will be given by means of a real quaternion product and matrix forms of homothetic motion.

Definition 4.1. Let $\alpha: I\subset\mathbb{R}\to\mathbb{R}^3$ be a regular space curve. Then, the surface $\Psi^{EL}(s,\theta)=\left(\Psi^{EL_1}(s,\theta),\Psi^{EL_2}(s,\theta),\Psi^{EL_3}(s,\theta)\right)$, which can be given by

$$\begin{aligned}\Psi^{EL}(s,\theta) &= \alpha(s)-\left(m^2+1\right)\sigma(s,\theta)\,\sigma(s,\theta)_s\,\vec{T}(s)\\ &\quad\pm\sqrt{m^2+1}\sigma(s,\theta)\sqrt{1-(m^2+1)\,\sigma(s,\theta)_s^2}(\cos\theta\vec{g}(s)+\sin\theta\vec{n}(s))\end{aligned} \tag{4.1}$$

is called an embankment-like surface, where $\left\{\vec{T},\vec{g},\vec{n}\right\}$ is the Darboux frame of $\alpha(s)$, $\sigma(s,\theta)=\Omega(s,\theta)-\alpha_3(s)$ and $m\in\mathbb{R}$, $m>0$ with $\left|m\alpha_3'\right|<\sqrt{\left(\alpha_1'\right)^2+\left(\alpha_2'\right)^2}$ and $\Omega(s,\theta)$ is an arbitrary function of s and θ.

Corollary 4.2. *Let $\alpha: I\subset\mathbb{R}\to\mathbb{R}^3$ be a unit speed diretrix curve of embankment-like surface $\Psi^{EL}(s,\theta)$ and $Q(s,\theta)=cos\frac{\theta}{2}+\sin\frac{\theta}{2}\vec{T}(s)$ be a unit real quaternion in $S^3\subset\mathbb{R}^4$. Then, the parametric equation of embankment-like surface $\Psi^{EL}(s,\theta)$ generated by the curve α can be given.*

(*i*) Via the real quaternion product $Q(s,\theta)\times\vec{g}(s)\times Q^{-1}(s,\theta)$,

$$\begin{aligned}\Psi^{EL}(s,\theta) &= \alpha(s)-\left(m^2+1\right)\sigma(s,\theta)\,\sigma(s,\theta)_s\,\vec{T}(s)\\ &\quad\pm\sqrt{m^2+1}\sigma(s,\theta)\sqrt{1-(m^2+1)\,\sigma(s,\theta)_s^2}Q(s,\theta)\times\vec{g}(s)\times Q^{-1}(s,\theta).\end{aligned} \tag{4.2}$$

(*ii*) Via the matrix representation of the map, $\phi:\mathbb{R}^3\to\mathbb{R}^3$ for the unit real quaternion $Q(s,\theta)$ and $\Psi^{EL}(s,\theta)$ can be obtained by the homothetic motion as

$$\begin{aligned}\Psi^{EL}(s,\theta) &= \alpha(s)-\left(m^2+1\right)\sigma(s,\theta)\,\sigma(s,\theta)_s\,\vec{T}(s)\\ &\quad\pm\sqrt{m^2+1}\sigma(s,\theta)\sqrt{1-(m^2+1)\,\sigma(s,\theta)_s^2}\mathcal{M}_Q g,\end{aligned} \tag{4.3}$$

where $\left\{\vec{T},\vec{g},\vec{n}\right\}$ is the Darboux frame of $\alpha(s)$, $\mathcal{M}_Q$ is the matrix representation of the map ϕ for $Q(s,\theta)$, $\sigma(s,\theta)=\Omega(s,\theta)-\alpha_3(s)$, $\Omega(s,\theta)$ is an arbitrary function of s, and θ , $m\in\mathbb{R}$, $m>0$ with $\left|m\alpha_3'\right|<\sqrt{\left(\alpha_1'\right)^2+\left(\alpha_2'\right)^2}$.

Proof. By choosing $\Psi^{E_3}(s,\theta)=\Omega(s,\theta)$ in Theorem 3.4 presented in Section 3, the proof becomes evident, where $\Omega(s,\theta)$ is an arbitrary function of s and θ. □

5. Tubembankment-like surfaces according to the Darboux frame in $\mathbf{E}^3$

In this section, we introduce a tubembankment-like surface, which represents another special case of embankment surfaces obtained from the nonzero constant function $\sigma(s,\theta) = c$. The parametric equations of these surfaces are then expressed in terms of the Darboux frame, using the real quaternion product and its matrix representation as a homothetic motion. For convenience in the computations of theorems and examples, the sign will be assumed positive. Similarly, calculations can also be carried out with the negative sign. Finally, the geometric properties of these surfaces are presented using the given theorems.

Definition 5.1. For the embankment-like surface given in (4.1), if $\sigma(s,\theta) = c$ is a constant function, this surface is called a tubembankment-like surface.

Corollary 5.2. *Let $\alpha : I \subset \mathbb{R} \to \mathbb{R}^3$ be a unit speed diretrix curve of an embankment-like surface $\Psi^{TEL}(s,\theta)$. Then, the parametrization of tubembankment-like surface generated by $\alpha(s)$ is given by*

$$\Psi^{TEL}(s,\theta) = \alpha(s) \pm c\sqrt{m^2+1}(\cos\theta\vec{g}(s) + \sin\theta\vec{n}(s)), \tag{5.1}$$

where $\left\{\vec{T},\vec{g},\vec{n}\right\}$ is the Darboux frame of $\alpha(s)$.

Corollary 5.3. *Let $\alpha : I \subset \mathbb{R} \to \mathbb{R}^3$ be a unit speed diretrix curve of a tubembankment-like surface $\Psi^{TEL}(s,\theta)$ and $Q(s,\theta) = cos\frac{\theta}{2} + \sin\frac{\theta}{2}\vec{T}(s)$ be a unit real quaternion in $S^3 \subset \mathbb{R}^4$. Then, the parametric equation of tubembankment-like surface $\Psi^{TEL}(s,\theta)$ generated by the curve α can be given.*

(*i*) Via the real quaternion product $Q(s,\theta) \times \vec{g}(s) \times Q^{-1}(s,\theta)$,

$$\Psi^{TEL}(s,\theta) = \alpha(s) \pm c\sqrt{m^2+1}Q(s,\theta) \times \vec{g}(s) \times Q^{-1}(s,\theta).$$

(*ii*) Via the matrix representation of the map, $\phi : \mathbb{R}^3 \to \mathbb{R}^3$ for the unit real quaternion $Q(s,\theta)$ and $\Psi^{TEL}(s,\theta)$ can be obtained by the homothetic motion as

$$\Psi^{TEL}(s,\theta) = \alpha(s) \pm c\sqrt{m^2+1}\mathcal{M}_Q g,$$

where $\left\{\vec{T},\vec{g},\vec{n}\right\}$ is the Darboux frame of $\alpha(s)$, $\mathcal{M}_Q$ is the matrix representation of the map ϕ for $Q(s,\theta)$, $\sigma(s,\theta) = c$ is constant function, and $m \in \mathbb{R}$, $m > 0$ with $\left|m\alpha_3'\right| < \sqrt{\left(\alpha_1'\right)^2 + \left(\alpha_2'\right)^2}$.

The unit normal vector $\vec{U}$ of the tubembankment-like surface is given as

$$\vec{U}(s,\theta) = \cos\theta\vec{g}(s) + \sin\theta\vec{n}(s). \tag{5.2}$$

The first and second order derivatives of the tubembankment-like surface $\Psi^{TEL}(s,\theta)$ with respect to the parameters s and θ can be easily calculated as follows:

$$
\begin{aligned}
\Psi_{s}^{TEL} &= A\vec{T}(s) - c\sqrt{m^2+1}\sin\theta\tau_g\vec{g}(s) + c\sqrt{m^2+1}\cos\theta\tau_g\vec{n}(s),\\
\Psi_{\theta}^{TEL} &= -c\sqrt{m^2+1}\sin\theta\vec{g}(s) + c\sqrt{m^2+1}\cos\theta\vec{n}(s),\\
\Psi_{ss}^{TEL} &= \Big(-c\sqrt{m^2+1}\,\kappa_g'\cos\theta - c\sqrt{m^2+1}\,\kappa_n'\sin\theta\\
&\quad +c\sqrt{m^2+1}\,\kappa_g\tau_g\sin\theta - c\sqrt{m^2+1}\,\kappa_n\tau_g\cos\theta\Big)\vec{T}(s)\\
&\quad +\Big(A\kappa_g - c\sqrt{m^2+1}\,\tau_g'\sin\theta - c\sqrt{m^2+1}\tau_g^2\cos\theta\Big)\vec{g}(s)\\
&\quad +\Big(A\kappa_n + c\sqrt{m^2+1}\,\tau_g'\cos\theta - c\sqrt{m^2+1}\tau_g^2\sin\theta\Big)\vec{n}(s),\\
\Psi_{s\theta}^{TEL} &= \Big(c\sqrt{m^2+1}\,\kappa_g\sin\theta - c\sqrt{m^2+1}\,\kappa_n\cos\theta\Big)\vec{T}(s)\\
&\quad - c\sqrt{m^2+1}\tau_g\cos\theta\vec{g}(s) - c\sqrt{m^2+1}\tau_g\sin\theta\vec{n}(s),\\
\Psi_{\theta\theta}^{TEL} &= -c\sqrt{m^2+1}\cos\theta\vec{g}(s) - c\sqrt{m^2+1}\sin\theta\vec{n}(s).
\end{aligned}
\tag{5.3}
$$

In order to find the surface properties of the tubembankment-like surface, it is useful to have expressions for the coefficients of the first and second fundamental forms given by

$$
\begin{aligned}
g_{11} &= A^2 + c^2\left(m^2+1\right)\tau_g^2, g_{12} = c^2\left(m^2+1\right)\tau_g, g_{22} = c^2\left(m^2+1\right),\\
L_{11} &= A\left(\kappa_g\cos\theta + \kappa_n\sin\theta\right) - c\sqrt{m^2+1}\tau_g^2, L_{12} = -c\sqrt{m^2+1}\tau_g, L_{22} = -c\sqrt{m^2+1}.
\end{aligned}
\tag{5.4}
$$

The Gauss and mean curvature functions of the tubembankment-like surface are given as follows:

$$
\begin{aligned}
K &= -\frac{\kappa_g\cos\theta + \kappa_n\sin\theta}{Ac\sqrt{m^2+1}},\\
H &= \frac{c\sqrt{m^2+1}\left(\kappa_g\cos\theta + \kappa_n\sin\theta\right) - A}{2Ac\sqrt{m^2+1}},\\
H &= -\frac{1}{2}\left(\frac{1}{c\sqrt{m^2+1}} + c\sqrt{m^2+1}K\right),
\end{aligned}
\tag{5.5}
$$

where $A = 1 - c\sqrt{m^2+1}\kappa_g\cos\theta - c\sqrt{m^2+1}\kappa_n\sin\theta$.

Proposition 5.4. *The tubembankment-like surface* $\Psi^{TEL}(s,\theta)$ *given by* (5.1) *is a regular surface if and only if the inequality* $\kappa_g\cos\theta + \kappa_n\sin\theta \neq \dfrac{1}{c\sqrt{m^2+1}}$ *is provided.*

Proof. The surface to be regular should provide inequality $g_{11}g_{22} - g_{12}^2 \neq 0$. By using (5.4), we have

$$g_{11}g_{22} - g_{12}^2 = A^2c^2\left(m^2+1\right),$$

where $A = 1 - c\sqrt{m^2+1}\kappa_g\cos\theta - c\sqrt{m^2+1}\kappa_n\sin\theta$.

Since c is a nonzero constant, $c^2\left(m^2+1\right) \neq 0$. So, from the last equation, we obtain

$$\kappa_g\cos\theta + \kappa_n\sin\theta \neq \frac{1}{c\sqrt{m^2+1}}.$$

So, the proof is completed. □

Theorem 5.5. *The Gaussian curvature function K of the regular tubembankment-like $\Psi^{TEL}(s,\theta)$ is zero if, and only if, $\tau_g = \tau$ for the s parameter curves.*

Proof. Let K be zero. Then,

$$K = \frac{\kappa_g \cos\theta + \kappa_n \sin\theta}{c^2\left(m^2+1\right)\kappa_g \cos\theta + c^2\left(m^2+1\right)\kappa_N \sin\theta - c\sqrt{m^2+1}} = 0.$$

Hence, we conclude that $\kappa_g \cos\theta + \kappa_n \sin\theta = 0$. It means that $\frac{\kappa_g}{\kappa_n}$ is constant for s parameter curves. We know that $\Theta = arccot\left(\frac{\kappa_g}{\kappa_n}\right)$ is constant. Since $\tau_g(s) = \tau(s) + \frac{d\Theta}{ds}$, therefore, we obtain $\tau_g = \tau$. The sufficiency part of the proof is obvious. □

Theorem 5.6. *Let $\Psi^{TEL}(s,\theta)$ be a regular tubembankment-like surface* (5.1) *in E^3. Section curves of the tubembankment-like surface $\Psi^{TEL}(s,\theta)$ have the following properties.*

(*i*) The s-parameter curve of the surface $\Psi^{TEL}(s,\theta)$ is an asymptotic curve if and only if the following equality is satisfied:

$$1 - c\sqrt{m^2+1}\kappa_g \cos\theta - c\sqrt{m^2+1}\kappa_n \sin\theta = \frac{c\sqrt{m^2+1}\tau_g^2}{\kappa_g \cos\theta + \kappa_n \sin\theta}. \tag{5.6}$$

(*ii*) The θ-parameter curve of the surface $\Psi^{TEL}(s,\theta)$ cannot be an asymptotic curve.

Proof. (*i*) A curve γ on a surface in E^3 is an asymptotic curve if, and only if, normal vector γ'' always points to the curve as tangent to the surface, that is, $\left\langle \vec{U}, \gamma'' \right\rangle = 0$. For the s-parameter curve, by using (5.2) and (5.3), we have

$$\begin{aligned} \left\langle \vec{U}, \Psi_{ss}^{TEL} \right\rangle &= \left(\kappa_g \cos\theta + \kappa_n \sin\theta\right)\left(1 - c\sqrt{m^2+1}\kappa_g \cos\theta - c\sqrt{m^2+1}\kappa_n \sin\theta\right) - c\sqrt{m^2+1}\tau_g^2 \\ &= 0. \end{aligned}$$

By making the necessary adjustments in this expression, equality (5.6) is obtained.

(*ii*) By using (5.2) and (5.3), the following inequality is provided

$$\left\langle \vec{U}, \Psi_{\theta\theta}^{TEL} \right\rangle = -c\sqrt{m^2+1} \neq 0,$$

for the θ-parameter curve, this curve cannot be an asymptotic curve. □

Theorem 5.7. *Let $\Psi^{TEL}(s,\theta)$ be a regular tubembankment-like surface* (5.1) *in E^3. Section curves of the tubembankment-like surface $\Psi^{TEL}(s,\theta)$ have the following properties.*

(*i*) The θ-parameter curve of the surface $\Psi^{TEL}(s,\theta)$ is a geodesic curve.

(*ii*) The s-parameter curve of the surface $\Psi^{TEL}(s,\theta)$ is a geodesic curve if, and only if, κ_g is constant, where $\theta \notin \left\{\frac{k\pi}{2} \,\middle|\, k \in \mathbb{Z}\right\}$. In addition, the condition of τ_g being constant requires $\frac{\kappa_n}{\kappa_g} = \tan\theta$.

Proof. (*i*) A curve γ lying on a surface is a geodesic curve if, and only if, the acceleration means that γ'' and the surface normal $\vec{U}$ are linearly dependent, namely, $\vec{U} \wedge \gamma'' = 0$. In this case, for the θ-parameter curve, by using (5.2) and (5.3), we get

$$\vec{U} \wedge \Psi_{\theta\theta}^{TEL} = 0.$$

Hence, the θ-parameter curve on the surface is always a geodesic curve.

(*ii*) For the s-parameter curve, by using (5.2) and (5.3), we compute

$$\begin{aligned}\vec{U} \wedge \Psi_{ss}^{TEL} &= \left[\left(\kappa_n \cos\theta - \kappa_g \sin\theta\right)\left(1 - c\sqrt{m^2+1}\kappa_g \cos\theta - c\sqrt{m^2+1}\kappa_n \sin\theta\right) + c\sqrt{m^2+1}\tau_g'\right]\vec{T}(s) \\ &+ \left[c\sqrt{m^2+1}\sin^2\theta\left(\kappa_g\tau_g - \kappa_n'\right) + c\sqrt{m^2+1}\sin\theta\cos\theta\left(\tau_g\kappa_n - \kappa_g'\right)\right]\vec{g}(s) \\ &+ \left[c\sqrt{m^2+1}\cos^2\theta\left(-\kappa_g' - \tau_g\kappa_n\right) + c\sqrt{m^2+1}\sin\theta\cos\theta\left(\kappa_n' - \kappa_g\tau_g\right)\right]\vec{n}(s).\end{aligned}$$

Since $\{\vec{T}, \vec{g}, \vec{n}\}$ is a triply orthogonal system and $\vec{U} \wedge \Psi_{ss}^{TEL} = 0$, the following equalities are obtained

$$\begin{cases} \left[\left(\kappa_n \cos\theta - \kappa_g \sin\theta\right)\left(1 - c\sqrt{m^2+1}\kappa_g \cos\theta - c\sqrt{m^2+1}\kappa_n \sin\theta\right) + c\sqrt{m^2+1}\tau_g'\right] = 0, \\ \left[c\sqrt{m^2+1}\sin^2\theta\left(\kappa_g\tau_g - \kappa_n'\right) + c\sqrt{m^2+1}\sin\theta\cos\theta\left(\tau_g\kappa_n - \kappa_g'\right)\right] = 0, \\ \left[c\sqrt{m^2+1}\cos^2\theta\left(-\kappa_g' - \tau_g\kappa_n\right) + c\sqrt{m^2+1}\sin\theta\cos\theta\left(\kappa_n' - \kappa_g\tau_g\right)\right] = 0. \end{cases}$$

By the last two equations, the second equation is multiplied by $\cos\theta$ and the third equation multiplied by $\sin\theta$, then they are added together and necessary adjustments are made, and we obtain κ_g is constant. Also considering the first equation, the following equality is obtained.

$$\tau_g' = -\frac{\left(\kappa_n \cos\theta - \kappa_g \sin\theta\right)\left(1 - c\sqrt{m^2+1}(\kappa_g \cos\theta + \kappa_n \sin\theta)\right)}{c\sqrt{m^2+1}}.$$

Since the surface is regular, then, we know

$$\kappa_g \cos\theta + \kappa_n \sin\theta \neq \frac{1}{c\sqrt{m^2+1}}.$$

Therefore, the condition of τ_g being constant requires $\kappa_n \cos\theta - \kappa_g \sin\theta = 0$. In other words, it necessitates $\frac{\kappa_n}{\kappa_g} = \tan\theta$. Then, the proof is completed. □

Proposition 5.8. *[35] On the surface, a hyperbolic point is a minimal point if, and only if, the coefficients of the first and second fundamental forms at this point are satisfying the following equation:*

$$g_{22}L_{11} - 2g_{12}L_{12} + g_{11}L_{22} = 0. \tag{5.7}$$

Theorem 5.9. *The minimal curves of regular tubembankment-like surface given by* (5.8)

$$\Psi^{TEL}(s,\theta) = \alpha(s) + c\sqrt{m^2+1}(\cos\theta\vec{g}(s) + \sin\theta\vec{n}(s)) \tag{5.8}$$

are as follows:

$$\beta(s) = \alpha(s) + c\sqrt{m^2+1}(\cos\theta\vec{g}(s) + \sin\theta\vec{n}(s)), \tag{5.9}$$

where $\theta = \int\left(\tau_g(s) - \tau(s)\right)ds + \arccos\left(\frac{1}{2\kappa(s)\,c\sqrt{m^2+1}}\right)$, $\kappa \neq 0$, and, here, κ and τ are the curvature functions of the curve $\alpha(s)$.

Proof. From (5.4) and (5.7), we have

$$2c\sqrt{m^2+1}\left(\kappa_g\cos\theta+\kappa_n\sin\theta\right)-1=0.$$

Therefore, we obtain

$$\cos\left(\theta-\Theta\right)=\left(\frac{1}{2\kappa\left(s\right)c\sqrt{m^2+1}}\right),$$

and so,

$$\theta=\int\left(\tau_g\left(s\right)-\tau\left(s\right)\right)ds+\arccos\left(\frac{1}{2\kappa\left(s\right)c\sqrt{m^2+1}}\right),$$

where $\kappa_g\left(s\right)=\kappa\left(s\right)\cos\Theta\left(s\right)$, $\kappa_n\left(s\right)=\kappa\left(s\right)\sin\Theta\left(s\right)$, and $\tau_g\left(s\right)=\tau(s)+\dfrac{d\Theta}{ds}$. This completes the proof. □

Theorem 5.10. *If $\alpha\left(s\right):I\subset\mathbb{R}\to\mathbb{R}^3$ is a regular unit speed space curve with nonzero curvature, then the tubembankment-like surface $\Psi^{TEL}\left(s,\theta\right)$ given by* (5.1) *, with directrix curve $\alpha\left(s\right)$ and a non-degenerate second fundamental form, is a (H,K)-Weingarten surface.*

Proof. By the help of (5.5), we know that

$$H=-\frac{1}{2}\left(\frac{1}{c\sqrt{m^2+1}}+c\sqrt{m^2+1}K\right).$$

From this, we can easily check that $H_sK_\theta-H_\theta K_s=0$. Thus, the tubembankment-like surface $\Psi^{TEL}\left(s,\theta\right)$ is a (H,K)-Weingarten surface. □

6. Visualizations for embankment-like and tubembankment-like surface in $\mathbf{E}^3$

In this section, we present examples of embankment-like and tubembankment-like surfaces generated by the unit speed curve $\alpha\left(s\right)$ with respect to the Darboux frame. For these examples, we assume the positive sign; however, the same construction can be carried out with the negative sign as well. Thereafter, we provide the parametric equations of these surfaces, followed by their quaternionic and matrix representations. Finally, we illustrate their graphs using the software Mathematica.

Consider the surface of the cylinder Γ given by the parametrization $\Gamma(u,v)=(\sin u,\cos u,v)$. The curve given by the parametrization form $\alpha(s)=\left(\sin\dfrac{s}{\sqrt{2}},\cos\dfrac{s}{\sqrt{2}},\dfrac{s}{\sqrt{2}}\right)$ is a unit speed helix curve on the surface Γ. The curve $\alpha(s)$ is regarded with respect to the components of the Darboux frame as:

$$\alpha(s)=\left\langle\alpha(s),\vec{T}(s)\right\rangle\vec{T}(s)+\left\langle\alpha(s),\vec{g}(s)\right\rangle\vec{g}(s)+\left\langle\alpha(s),\vec{n}(s)\right\rangle\vec{n}(s)).\tag{6.1}$$

To simplify the notation, the curve $\alpha(s)$ with respect to the Darboux frame will be denoted by $\beta(s)$.

Vector fields and curvatures of the Darboux frame $\left\{\vec{T},\vec{g},\vec{n},\kappa_n,\kappa_g,\tau_g\right\}$ of the curve $\alpha\left(s\right)$ can be calculated as follows:

$$\vec{T}(s)\;\;=\;\;(t_1,t_2,t_3)=\frac{1}{\sqrt{2}}\left(\cos\frac{s}{\sqrt{2}},-\sin\frac{s}{\sqrt{2}},1\right)$$

$$\begin{aligned}\vec{g}(s) &= \frac{1}{\sqrt{2}}\left(-\cos\frac{s}{\sqrt{2}}, \sin\frac{s}{\sqrt{2}}, 1\right)\\ \vec{n}(s) &= \left(-\sin\frac{s}{\sqrt{2}}, -\cos\frac{s}{\sqrt{2}}, 0\right)\\ \kappa_n &= 0,\ \kappa_g = -\frac{1}{2},\ \tau_g = -\frac{1}{2}.\end{aligned}$$

Throughout the matrix multiplications, the vector $\vec{g}(s)$ is consistently treated as a 3×1 column matrix and will be denoted by g. The given vector is considered as a pure quaternion in the quaternion multiplications. The following equality, also theoretically proven in Eq (3.18) of Section 3, is known to facilitate the representation of the examples in terms of homothetic motions and quaternions with respect to the Darboux frame

$$\mathcal{M}_Q g = Q(s,\theta) \times \vec{g}(s) \times Q^{-1}(s,\theta) = \cos\theta\vec{g}(s) + \sin\theta\vec{n}(s). \tag{6.2}$$

Moreover, $\mathcal{M}_Q$ is a matrix equivalent to the unit real quaternion $Q(s,\theta) = cos\frac{\theta}{2} + \sin\frac{\theta}{2}\vec{T}(s)$ given as the following:

$$\mathcal{M}_Q = \begin{bmatrix} a_{11} & a_{12} & a_{13} \\ a_{21} & a_{22} & a_{23} \\ a_{31} & a_{32} & a_{33} \end{bmatrix} \tag{6.3}$$

$$\mathcal{M}_Q = \begin{bmatrix} \cos^2\frac{\theta}{2} + \sin^2\frac{\theta}{2}\left(t_1^2 - t_2^2 - t_3^2\right) & -t_3\sin\theta + 2t_1t_2\sin^2\frac{\theta}{2} & t_2\sin\theta + 2t_1t_3\sin^2\frac{\theta}{2} \\ t_3\sin\theta + 2t_1t_2\sin^2\frac{\theta}{2} & \cos^2\frac{\theta}{2} + \sin^2\frac{\theta}{2}\left(t_2^2 - t_1^2 - t_3^2\right) & -t_1\sin\theta + 2t_2t_3\sin^2\frac{\theta}{2} \\ -t_2\sin\theta + 2t_1t_3\sin^2\frac{\theta}{2} & t_1\sin\theta + 2t_2t_3\sin^2\frac{\theta}{2} & \cos^2\frac{\theta}{2} + \sin^2\frac{\theta}{2}\left(t_3^2 - t_1^2 - t_2^2\right) \end{bmatrix}.$$

The first column of $\mathcal{M}_Q$ is given as

$$\begin{bmatrix} a_{11} \\ a_{21} \\ a_{31} \end{bmatrix} = \begin{bmatrix} \cos^2\frac{\theta}{2} + \frac{1}{2}\sin^2\frac{\theta}{2}\left(\cos\sqrt{2}s - 1\right) \\ \frac{1}{\sqrt{2}}\sin\theta - \frac{1}{2}\sin^2\frac{\theta}{2}\sin\sqrt{2}s \\ \frac{1}{\sqrt{2}}\sin\theta\sin\frac{s}{\sqrt{2}} + \sin^2\frac{\theta}{2}\cos\frac{s}{\sqrt{2}} \end{bmatrix},$$

the second column of $\mathcal{M}_Q$ is given as

$$\begin{bmatrix} a_{12} \\ a_{22} \\ a_{32} \end{bmatrix} = \begin{bmatrix} -\frac{1}{\sqrt{2}}\sin\theta - \frac{1}{2}\sin^2\frac{\theta}{2}\sin\sqrt{2}s \\ \cos^2\frac{\theta}{2} - \frac{1}{2}\sin^2\frac{\theta}{2}\left(\cos\sqrt{2}s + 1\right) \\ \frac{1}{\sqrt{2}}\sin\theta\cos\frac{s}{\sqrt{2}} - \sin^2\frac{\theta}{2}\sin\frac{s}{\sqrt{2}} \end{bmatrix},$$

and third column of $\mathcal{M}_Q$ is given as

$$\begin{bmatrix} a_{13} \\ a_{23} \\ a_{33} \end{bmatrix} = \begin{bmatrix} -\frac{1}{\sqrt{2}} \sin\theta \sin\frac{s}{\sqrt{2}} + \sin^2\frac{\theta}{2}\cos\frac{s}{\sqrt{2}} \\ -\frac{1}{\sqrt{2}} \sin\theta \cos\frac{s}{\sqrt{2}} - \sin^2\frac{\theta}{2}\sin\frac{s}{\sqrt{2}} \\ \cos^2\frac{\theta}{2} \end{bmatrix}.$$

Example 6.1. *Let's consider that* $\Omega(s,\theta) = \theta + \frac{s}{\sqrt{2}}, m = \frac{1}{2}$. *Then, we can construct the embankment-like surface. By the help of* (4.1) *we can easily obtain the equation of this surface by using components of the Darboux frame as*

$$\Psi^{EL}(s,\theta) = \beta(s) + \frac{\sqrt{5}\theta}{2}(\cos\theta\vec{g}(s) + \sin\theta\vec{n}(s)). \tag{6.4}$$

Employing the representation of the curve with respect to the Darboux frame together with its components yields the following equations:

(*i*) The parametric form of the embankment-like surface is given by:

$$\Psi^{EL}(s,\theta) = \begin{pmatrix} \sin\frac{s}{\sqrt{2}} - \frac{\sqrt{10}}{4}\theta\cos\theta\cos\frac{s}{\sqrt{2}} - \frac{\sqrt{5}}{2}\theta\sin\theta\sin\frac{s}{\sqrt{2}}, \\ \cos\frac{s}{\sqrt{2}} + \frac{\sqrt{10}}{4}\theta\cos\theta\sin\frac{s}{\sqrt{2}} - \frac{\sqrt{5}}{2}\theta\sin\theta\cos\frac{s}{\sqrt{2}}, \\ \frac{s}{\sqrt{2}} + \frac{\sqrt{10}}{4}\theta\cos\theta \end{pmatrix}.$$

(*ii*) As quaternionic via (6.2) and (6.4):

$$\Psi^{EL}(s,\theta) = \beta(s) + \frac{\sqrt{5}\theta}{2}Q(s,\theta)\times\vec{g}(s)\times Q^{-1}(s,\theta),$$

where $Q(s,\theta) = cos\frac{\theta}{2} + \sin\frac{\theta}{2}\vec{T}(s)$ is a unit real quaternion.

(*iii*) As a homothetic motion represented via the matrix form of $Q(s,\theta)$ according to (6.2) and (6.4):

$$\Psi^{EL}(s,\theta) = \beta(s) + \frac{\sqrt{5}\theta}{2}\mathcal{M}_Q g,$$

where $\mathcal{M}_Q$ (6.3) is a matrix equivalent of the unit real quaternion $Q(s,\theta)$.

The graph of this surface can be found in Figure 2 for the different parameters. In Figure 2(a), $s \in [-\pi,\pi]$ and $\theta \in [-5,5]$. In Figure 2(b), $s \in [-3,3]$ and $\theta \in \left[-\frac{3\pi}{2}, \frac{3\pi}{2}\right]$. In Figure 2(c), $s \in [-5,5]$ and $\theta \in [-2,2]$. Distortions in the surface plots are particularly evident in Figure a, where the regularity of the surfaces is not maintained.

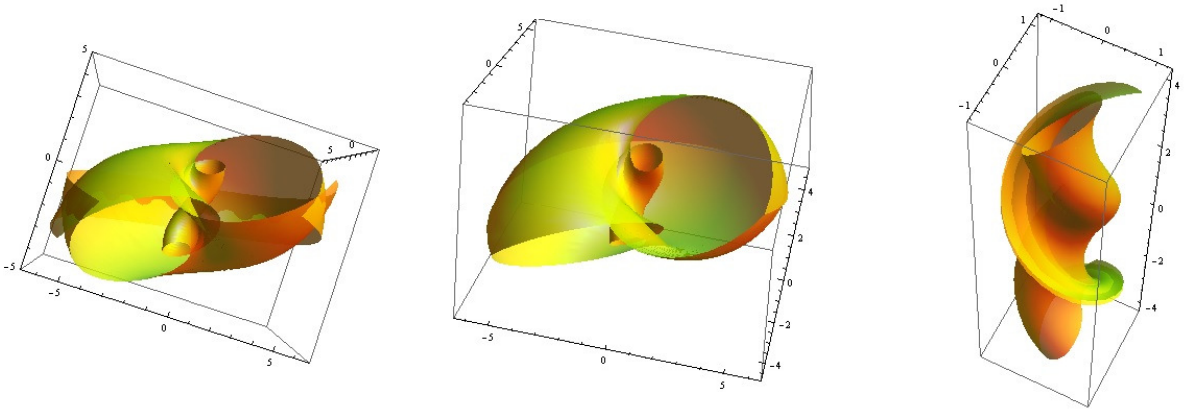

(a) **(b)** **(c)**

Figure 2. Embankment-like surface $\Psi^{EL}(s,\theta)$.

Example 6.2. *Let's consider that* $\Omega(s,\theta) = \theta, m = \frac{1}{2}$. *Then, we can construct the embankment-like surface. By the help of* (4.1)*, we can easily obtain the equation of this surface by using components of the Darboux frame as*

$$\Psi^{EL}(s,\theta) = \beta(s) + \frac{5\sqrt{2}}{8}\left(\theta - \frac{s}{\sqrt{2}}\right)\vec{T}(s) + \frac{\sqrt{30}}{8}\left(\theta - \frac{s}{\sqrt{2}}\right)(\cos\theta\vec{g}(s) + \sin\theta\vec{n}(s)). \tag{6.5}$$

By utilizing the representation of the curve in the Darboux frame along with its components, one arrives at the following equations:

(*i*) The parametric form of the embankment-like surface is given by:

$$\Psi^{EL}(s,\theta) = \begin{pmatrix} \sin\frac{s}{\sqrt{2}} + \frac{5}{8}\left(\theta - \frac{s}{\sqrt{2}}\right)\cos\frac{s}{\sqrt{2}} - \frac{\sqrt{15}}{8}\left(\theta - \frac{s}{\sqrt{2}}\right)\cos\theta\cos\frac{s}{\sqrt{2}} \\ -\frac{\sqrt{30}}{8}\left(\theta - \frac{s}{\sqrt{2}}\right)\sin\theta\sin\frac{s}{\sqrt{2}}, \\ \cos\frac{s}{\sqrt{2}} - \frac{5}{8}\left(\theta - \frac{s}{\sqrt{2}}\right)\sin\frac{s}{\sqrt{2}} + \frac{\sqrt{15}}{8}\left(\theta - \frac{s}{\sqrt{2}}\right)\cos\theta\sin\frac{s}{\sqrt{2}} \\ -\frac{\sqrt{30}}{8}\left(\theta - \frac{s}{\sqrt{2}}\right)\sin\theta\cos\frac{s}{\sqrt{2}}, \\ \frac{s}{\sqrt{2}} + \frac{5}{8}\left(\theta - \frac{s}{\sqrt{2}}\right) + \frac{\sqrt{15}}{8}\left(\theta - \frac{s}{\sqrt{2}}\right)\cos\theta \end{pmatrix}.$$

(*ii*) As quaternionic via (6.2) and (6.5):

$$\Psi^{EL}(s,\theta) = \beta(s) + \frac{5\sqrt{2}}{8}\left(\theta - \frac{s}{\sqrt{2}}\right)\vec{T}(s) + \frac{\sqrt{30}}{8}\left(\theta - \frac{s}{\sqrt{2}}\right)Q(s,\theta)\times\vec{g}(s)\times Q^{-1}(s,\theta),$$

where $Q(s,\theta) = cos\frac{\theta}{2} + \sin\frac{\theta}{2}\vec{T}(s)$ is a unit real quaternion.

(*iii*) As a homothetic motion represented via the matrix form of $Q(s,\theta)$ according to (6.2) and (6.5):

$$\Psi^{EL}(s,\theta) = \beta(s) + \frac{5\sqrt{2}}{8}\left(\theta - \frac{s}{\sqrt{2}}\right)\vec{T}(s) + \frac{\sqrt{30}}{8}\left(\theta - \frac{s}{\sqrt{2}}\right)\mathcal{M}_{Q}g,$$

where $\mathcal{M}_Q$ (6.3) is a matrix equivalent of the unit real quaternion $Q(s,\theta)$.

The graphs of this surface for different parameters can be found in Figure 3. In Figure 3(a), $s \in [-\pi,\pi]$ and $\theta \in [-5,5]$. In Figure 3(b), $s \in [\pi,\pi]$ and $\theta \in [-4\pi,4\pi]$. In Figure 3(c), $s \in [-3\pi,3\pi]$ and $\theta \in [-10\pi,10\pi]$. Distortions in the surface plots are observed in Figure 3, where the regularity of the surfaces is not maintained.

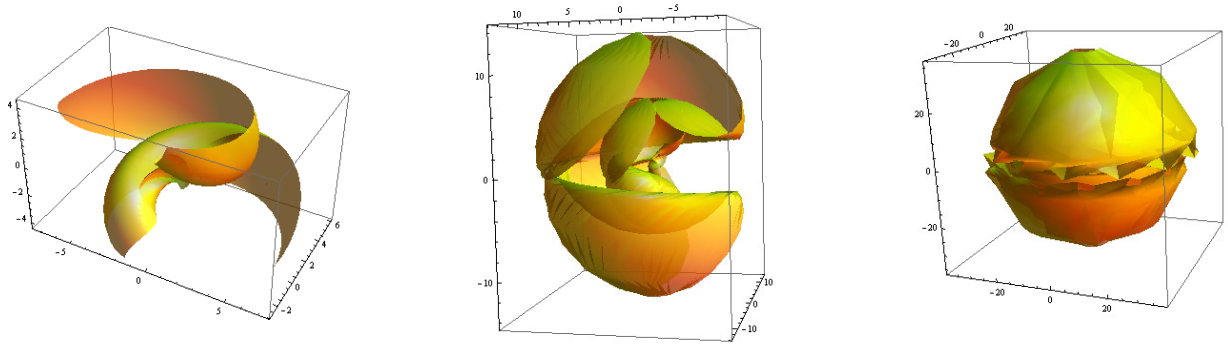

(a) **(b)** **(c)**

Figure 3. Embankment-like surface $\Psi^{EL}(s,\theta)$.

Example 6.3. *Let's consider that* $\sigma(s,\theta) = 1, m = \frac{3}{4}$. *Then, we can construct the tubembankment-like surface as the following. By the help of* (5.1)*, we can easily obtain the equation of this surface by using components of Darboux frame as*

$$\Psi^{TEL}(s,\theta) = \beta(s) + \frac{5}{4}(\cos\theta\vec{g}(s) + \sin\theta\vec{n}(s)). \tag{6.6}$$

Using the Darboux frame representation of the curve in conjunction with its components leads to the following equations:

(*i*) The parametric form of the embankment-like surface is given by:

$$\Psi^{TEL}(s,\theta) = \begin{pmatrix} \sin\frac{s}{\sqrt{2}} - \frac{5\sqrt{2}}{8}\cos\theta\cos\frac{s}{\sqrt{2}} - \frac{5}{4}\sin\theta\sin\frac{s}{\sqrt{2}} \\ \cos\frac{s}{\sqrt{2}} + \frac{5\sqrt{2}}{8}\cos\theta\sin\frac{s}{\sqrt{2}} - \frac{5}{4}\sin\theta\cos\frac{s}{\sqrt{2}} \\ \frac{s}{\sqrt{2}} + \frac{5\sqrt{2}}{8}\cos\theta \end{pmatrix}.$$

(*ii*) As quaternionic via (6.2) and (6.6):

$$\Psi^{TEL}(s,\theta) = \beta(s) + \frac{5}{4}Q(s,\theta)\times\vec{g}(s)\times Q^{-1}(s,\theta),$$

where $Q(s,\theta) = cos\frac{\theta}{2} + \sin\frac{\theta}{2}\vec{T}(s)$ is a unit real quaternion.

(*iii*) As a homothetic motion represented via the matrix form of $Q(s,\theta)$ according to (6.2) and (6.6):

$$\Psi^{TEL}(s,\theta) = \beta(s) + \frac{5}{4}\mathcal{M}_Q g,$$

where $\mathcal{M}_Q$ (6.3) is a matrix equivalent of the unit real quaternion $Q(s,\theta)$.

Moreover, the Gauss and mean curvature of surface $\Psi^{TEL}(s,\theta)$ are given as:

$$K = \frac{16\cos\theta}{40 + 25\cos\theta},\ H = \frac{-16 - 20\cos\theta}{40 + 25\cos\theta}.$$

In addition, by applying the minimal curve condition stated in Theorem 5.9, we obtain $\theta = a + \arccos\frac{4}{5}$, where a is a real constant.

The graphs of this surface for different parameters can be found in Figure 4. In Figure 4(a), $s \in [-3,3]$ and $\theta \in [-4,4]$. In Figure 4(b), $s \in [-2\pi, 2\pi]$ and $\theta \in [-5\pi, 5\pi]$. In Figure 4(c), $s \in [-10,10]$ and $\theta \in [-5,5]$. Moreover, the minimal curve corresponding to the constant $\theta = \arccos\frac{4}{5}$ on the tubembankment-like surface is depicted in red. The endpoints of the curve are highlighted with blue points for clarity.

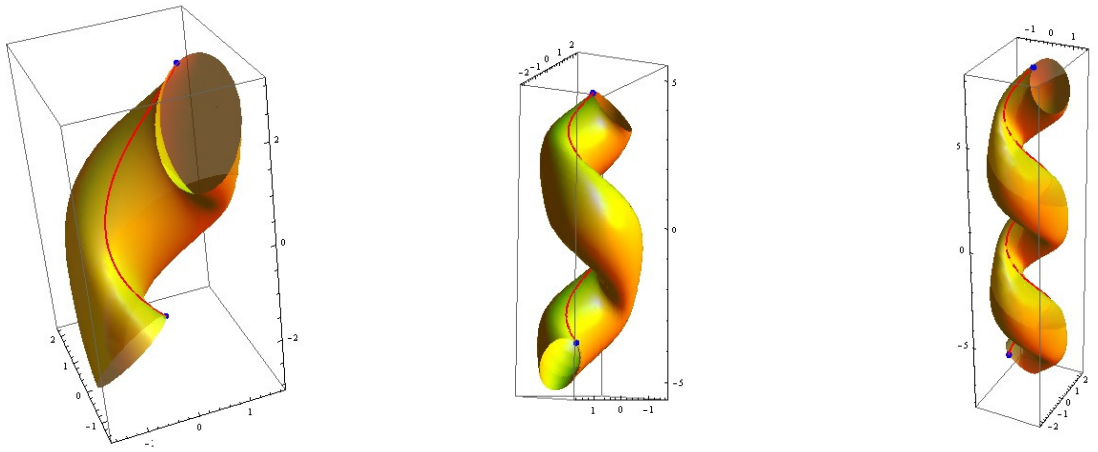

(a) **(b)** **(c)**

Figure 4. Tubembankment-like surface $\Psi^{TEL}(s,\theta)$ and its minimal curve.

Furthermore, the Gauss and mean curvature functions of the surface Ψ^{TEL} are presented in Figure 5. In this figure, the Gauss curvature function K is depicted by the red curve, while the mean curvature function H is represented by the blue curve. The Gauss and mean curvature functions are important for interpreting the flatness and minimality of the surface, respectively. Therefore, the graph presented in Figure 5 allows us to observe these properties.

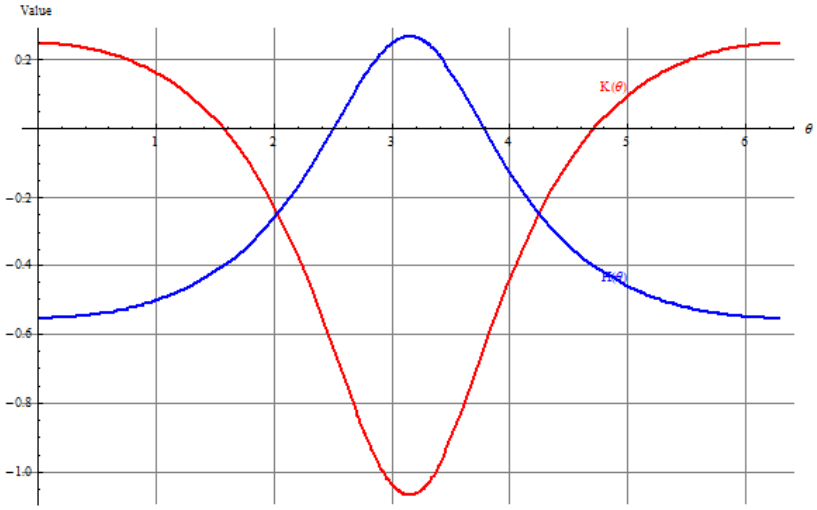

Figure 5. Gauss and mean curvature functions of the surface $\Psi^{TEL}(s,\theta)$.

7. Conclusions

In recent years, many researchers have studied canal and tubular surfaces using the Darboux frame. The concept of the embankment surface has been introduced more recently, with relatively few studies available. In this paper, we investigate the characterization of embankment, embankment-like, and tubembankment-like surfaces generated by a spatial curve with respect to the Darboux frame. Parametric definitions are provided, enabling the examination of geometric properties such as slope, curvature, durability, material compatibility, and drainage performance, which are crucial in engineering applications. The equations of these surfaces are simplified using matrix representations and quaternions, significantly reducing computational complexity. For tubembankment-like surfaces, curvature properties and special curves are analyzed, and the necessary conditions for minimal curves are obtained. These results are important for ensuring accurate and efficient design in practical applications.

Furthermore, the surfaces are visualized using the software Mathematica, clearly revealing their structural features. Analytical equations alone may be insufficient for full comprehension, whereas graphical visualization offers a strong analytical tool for both theoretical research and applied design. The findings contribute new perspectives and construction methods to differential geometry.

Study limitations: At the points where the curvature κ of the space curve is zero, the Darboux frame cannot be defined. Thus, the study is limited at this stage, which poses a problem.

Future recommendations: The combined use of the Darboux frame and quaternions provide a robust framework for future studies. The presented methods and visualization techniques may inspire applications in computer graphics, kinematics, and surface modeling. Additionally, extending the study of such surfaces to different motion types or alternative geometric spaces, such as Minkowski or isotropic spaces, presents promising directions for further research.

Use of Generative-AI tools declaration

The author declares that Artificial Intelligence (AI) tools are not used in this article.

Acknowledgments

The author is very grateful to the anonymous referees for their detailed comments and valuable suggestions, which greatly improved the manuscript.

Conflict of interest

The author declares no conflict of interests.

References

1. G. Monge, *Géométrie descriptive*, 1 Eds., Paris: Gauthier-Villars Collection, 1795.
2. E. Catalan, Sur les surface réglées dont l'aire est un minimum, *J. Math. Pure. Appl.*, **7** (1842), 203–211.
3. E. Study, *Geometrie der dynamen*, Leibzig: Teubner, 1903.
4. S. Izumiya, N. Takeuchi, New special curves and developable surfaces, *Turk. J. Math.*, **28** (2004), 6.
5. D. W. Yoon, On the second Gaussian curvature of ruled surfaces in Euclidean 3-space, *Tamkang J. Math.*, **37** (2006), 221–226. https://doi.org/10.5556/j.tkjm.37.2006.167
6. G. Monge, *Application de l'analyse a la geometrie*, Paris: Bachelier, 1807.
7. A. Gray, *Modern differential geometry of curves and surfaces with mathematica*, 2 Eds., Boca Raton: CRC Press, 1998.
8. A. Gross, Analyzing generalized tubes, *Proceedings of SPIE*, **2354** (1994), 422–433. https://doi.org/10.1117/12.189111
9. A. Uçum, K. İlarslan, New types of canal surfaces in Minkowski 3-space, *Adv. Appl. Clifford Algebras*, **26** (2016), 449–468. http://doi.org/10.1007/s00006-015-0556-7
10. Z. Q. Xu, R. Z. Feng, J.-G. Sun, Analytic and algebraic properties of canal surfaces, *Appl. Math. Comput.*, **195** (2006), 220–228. https://doi.org/10.1016/j.cam.2005.08.002
11. M. K. Karacan, Y. Yaylı, On the geodesics of tubular surfaces in Minkowski 3-space, *Bull. Malays. Math. Sci. Soc.*, **31** (2008), 1–10.
12. M. K. Karacan, Y. Tunçer, Tubular surfaces of Weingarten types in Galilean and pseudo-Galilean, *Bull. Math. Anal. Appl.*, **5** (2013), 87–100.
13. T. Maekawa, M. N. Patrikalakis, T. Sakkalis, G. X. Yu, Analysis and applications of pipe surfaces, *Comput. Aided Geom. D.*, **15** (1998), 437–458. https://doi.org/10.1016/S0167-8396(97)00042-3
14. P. A. Blaga, On tubular surfaces in computer graphics, *Studia Universitatis Babeș-Bolyai Informatica*, **50** (2005), 81–90.

15. F. Doğan, Y. Yaylı, Tubes with Darboux frame, *Int. J. Contemp. Math. Sciences*, **7** (2012), 751–758.
16. M. Kazaz, H. H. Uğurlu, M. Önder, S. Oral, Bertrand partner D-curves inthe Euclidean 3-space E^3, *AKU J. Sci. Eng.*, **16** (2016), 76–83. https://doi.org/10.5578/fmbd.25270
17. A. Yavuz, F. Ateş, Y. Yaylı, Ruled surfaces with constant slope ruling according to Darboux frame, *Mathematical Sciences and Applications E-Notes*, **8** (2020), 135–144. https://doi.org/10.36753/mathenot.640345
18. A. Yildirim, F. Kaya, Mannheim partner curves according to Darboux frame in the Euclidean 3-space $\mathbb{E}^3$, *Mathematical Sciences and Applications E-Notes*, **8** (2020), 54–59. https://doi.org/10.36753/mathenot.599866
19. W. R. Hamilton, On quaternions; or on a new system of imagniaries in algebra, *Philos. Mag.*, **25** (1844), 10–13. https://doi.org/10.1080/14786444408644923
20. H. H. Hacısalihoğlu, *Hareket geometrisi ve kuaterniyonlar teorisi*, Gazi: Gazi Univ. Press, 1983.
21. M. Özdemir, *Kuaterniyonlar ve geometri*, İzmir: Altın Nokta Yayınevi, 2020.
22. M. Babaarslan, Y. Yaylı, A new approach to constant slope surfaces with quaternion, *International Scholarly Research Notices*, **2012** (2012), 126358. https://doi.org/10.5402/2012/126358
23. S. Aslan, Y. Yaylı, Canal surfaces with quaternions, *Adv. Appl. Clifford Algebras*, **26** (2016), 31–38. http://doi.org/10.1007/s00006-015-0602-5
24. İ. Gök, Quaternionic approach of canal surfaces constructed by some new ideas, *Adv. Appl. Clifford Algebras*, **27** (2017), 1175–1190. http://doi.org/10.1007/s00006-016-0703-9
25. F. Doğan, Generalized canal surfaces, PhD Thesis, Ankara University, 2012.
26. F. Ateş, E. Kocakuşaklı, İ. Gök, Y. Yaylı, A study of the tubular surfaces constructed by the spherical indicatrices in Euclidean 3-space, *Turk. J. Math.*, **42** (2018), 1711–1725. http://doi.org/10.3906/mat-1610-101
27. E. Hartman, *Geometry and algorithms for computer aided design*, Darmstadt University of Technology, 2003.
28. *Geotechnical engineering manual: guidelines for embankment construction*, Department of Transportation Geotechnical Engineering Bureau, State of New York, 2015.
29. A. Kazan, H. B. Karadağ, Embankment surfaces in Euclidean 3-space and their visualizations, *Commun. Math. Appl.*, **10** (2019), 617–636. https://doi.org/10.26713/cma.v10i3.916
30. W. M. Mahmoud, S. M. Abd ElHafez,Weingarten isotropic embankment surfaces according to adapted frame, *Information Sciences Letters*, **11** (2022), 61–68. https://doi.org/10.18576/isl/110108
31. M. P. do Carmo, *Differential geometry of curves and surfaces*, New York: Prentice Hall, 1976.
32. J. S. Ro, D. W. Yoon, Tubes of Weingarten types in a Euclidean 3-space, *Journal of the Chungcheong Mathematical Society*, **22** (2009), 360–366. https://doi.org/10.14403/jcms.2014.27.3.403
33. B. O'Neill, *Elemantery differential geometry*, New York: Academic Press, 1966.
34. D. J. Struik, *Lectures on classical differential geometry*, 2 Eds., New York: Dover Publications, 1988.

35. F. Şemin, *Differential geometry I*, İstanbul: İstanbul University Press, 1983.

AIMS Press